Longfang Zou, Martin López-García, Withawat Withayachumnankul, Charan M. Shah, Arnan Mitchell, Madhu Bhaskaran, Sharath Sriram, Ruth Oulton, Maciej Klemm, and Christophe Fumeaux
Spectral and angular characteristics of dielectric resonator metasurface at optical frequencies
Applied Physics Letters, 2014; 105(19):191109-1-191109-4

AIP | Applied Physics Letters

Spectral and angular characteristics of dielectric resonator metasurface at optical frequencies

Longfang Zou, Martin López-García, Withawat Withayachumnankul, Charan M. Shah, Arnan Mitchell, Madhu Bhaskaran, Sharath Sriram, Ruth Oulton, Maciej Klemm, and Christophe Fumeaux

Citation: Applied Physics Letters **105**, 191109 (2014); doi: 10.1063/1.4901735
View online: http://dx.doi.org/10.1063/1.4901735
View Table of Contents: http://scitation.aip.org/content/aip/journal/apl/105/19?ver=pdfcov
Published by the AIP Publishing

Spectral and angular characteristics of dielectric resonator metasurface at optical frequencies

Longfang Zou,[1,2] Martin López-García,[2] Withawat Withayachumnankul,[1] Charan M. Shah,[3] Arnan Mitchell,[3] Madhu Bhaskaran,[3] Sharath Sriram,[3] Ruth Oulton,[2] Maciej Klemm,[2] and Christophe Fumeaux[1,a)]

[1]*School of Electrical and Electronic Engineering, The University of Adelaide, Adelaide, SA 5005, Australia*
[2]*Department of Electrical and Electronic Engineering, The University of Bristol, Bristol, BS8 1TH, United Kingdom*
[3]*Functional Materials and Microsystems Research Group, School of Electrical and Computer Engineering, RMIT University, Melbourne VIC 3001, Australia*

(Received 29 August 2014; accepted 3 November 2014; published online 12 November 2014)

The capability of manipulating light at subwavelength scale has fostered the applications of flat metasurfaces in various fields. Compared to metallic structure, metasurfaces made of high permittivity low-loss dielectric resonators hold the promise of high efficiency by avoiding high conductive losses of metals at optical frequencies. This letter investigates the spectral and angular characteristics of a dielectric resonator metasurface composed of periodic sub-arrays of resonators with a linearly varying phase response. The far-field response of the metasurface can be decomposed into the response of a single grating element (sub-array) and the grating arrangement response. The analysis also reveals that coupling between resonators has a non-negligible impact on the angular response. Over a wide wavelength range, the simulated and measured angular characteristics of the metasurface provide a definite illustration of how different grating diffraction orders can be selectively suppressed or enhanced through antenna sub-array design. © *2014 AIP Publishing LLC*.
[http://dx.doi.org/10.1063/1.4901735]

The development of flat metasurfaces has recently become a flourishing research field that demonstrates the exciting functionality of nanostructures to manipulate and control light at subwavelength scale. Conventionally, optical components, such as lenses and waveplates, rely on a difference in optical path lengths for beamshaping. On the other hand, metasurfaces manipulate transmitted or reflected wavefronts by modifying their phase through local resonance.[1,22,23] This degree of freedom enables us to shape the wavefront in unusual ways at virtually any frequency range.[2,24] Therefore, flat metasurfaces not only have advantage of compactness but also open perspective for the creation of novel devices, with significant impact on various fields such as holography, imaging, sensing, communications, and high performance data processing.[3–5]

In general, metasurfaces are created from subwavelength resonant elements arranged with subwavelength periods on a planar surface. These resonant elements can impart phase discontinuities, ranging from 0 to 2π, to the incident waves. The local phase response can be adjusted by changing geometrical parameters such as size, shape, and orientation of the resonators. Under the effective medium consideration, the operation of metasurfaces can be interpreted by using the Huygens' principle, for which each point on the surface is treated as a new source of a spherical wave with a controllable phase response. As for metasurfaces operated in reflection, the design concept is closely related to the reflectarray theory developed in the microwave frequency range.[6]

Most existing metasurfaces are constructed from metallic resonators. However, as the operation frequency of metasurfaces approaches the visible regime, metals become lossy owing to the plasmonic effect.[7] As an alternative, high permittivity dielectric resonators operate via displacement currents instead of electric currents as in their metallic counterpart. Thus, they do not suffer from the Ohmic loss in metals.[7–9,21] Recently, metasurfaces based on dielectric resonators have attracted considerable research interests.[10–15] In our earlier study,[10] a dielectric resonator metasurface for beam deflection was experimentally validated for operation at a single wavelength of 633 nm. In this letter, the spectral and angular responses are experimentally observed via visible-light spectroscopy. Further, its observable responses are analyzed in relation to the diffraction and array theories.[16]

In brief, the metasurface is composed of cylindrical nano-size dielectric resonators patterned on a silver film. The dielectric resonators are made of TiO_2 (titanium dioxide), a material that combines manufacturability at nano-scale, high relative permittivity ($\epsilon_{r\parallel} = 8.29$ and $\epsilon_{r\perp} = 6.71$), and low loss ($\tan\delta = 0.01$) at the desired wavelength.[10] The phase of the reflected beam is controlled by varying the diameter of the dielectric resonators across the reflective surface. The phase response as a function of the resonator diameter can be determined from infinite uniform arrays as shown in Fig. 1(a). By properly designing the lattice size and dimensions of the resonators, the phase change can nearly cover a 360° cycle. Phase wrapping allows a periodic design consisting of sub-arrays, each with only a few resonators. In the realized design, six dielectric resonators with a lattice constant of 310 nm and height of 50 nm have been selected to form a sub-array with a phase gradient of $\Delta\phi = 60°$. The selected diameters of cylindrical resonators are indicated as the red dots in Fig. 1(a). As shown in Fig. 1(b), the gradient metasurface is designed for

a)Electronic mail: christophe.fumeaux@adelaide.edu.au

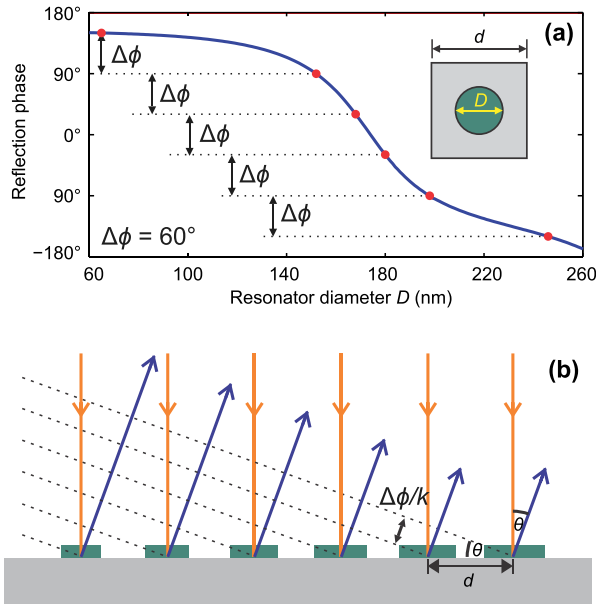

FIG. 1. (a) Numerically resolved phase responses of dielectric resonators at 633 nm wavelength. The responses vary as a function of the resonators diameter, for a fixed height of 50 nm and lattice constant of $d = 310$ nm. The dots indicate the selected diameters for a periodic metasurface made of 6-element sub-arrays. (b) Schematic of a deflected light wavefront manipulated by six resonators.

beam deflection at 19.9° away from specular reflection according to the equation derived from the reflectarray theory[17]

$$\sin\theta = \frac{\Delta\phi}{k_0 d}, \tag{1}$$

where θ is the deflection angle, k_0 is the free-space wavenumber at 633 nm, and d is the distance between the centres of two adjacent elements (i.e., lattice constant). Fig. 2(a) shows a render of the designed dielectric metasurface. A scanning electron micrograph of the fabricated metasurface is shown in Fig. 2(b), along with the actual dimensions. The maximum difference between designed and fabricated dielectric resonator dimensions is about 6%.

Because of the presence of the metallic plane, the dielectric resonators operate only in their magnetic dipole mode when excited by a normally incident plane wave, as shown in Fig. 3. This magnetic dipole mode is qualitatively similar to the fundamental $HEM_{11\delta}$ mode of a dielectric resonator at microwave frequencies.[18] However, whereas at microwave frequencies the metal plane can be modeled as a

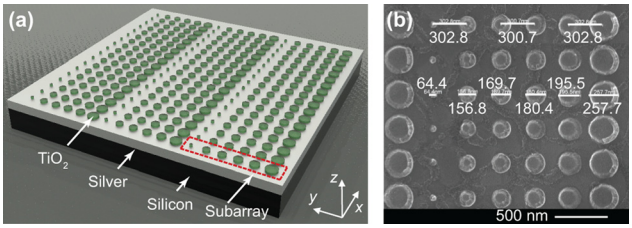

FIG. 2. (a) Schematic showing a partial view of a dielectric metasurface made of 6-element sub-arrays. (b) Scanning electron micrograph of fabricated metasurface with measured resonators size and lattice constant with a unit in nm.

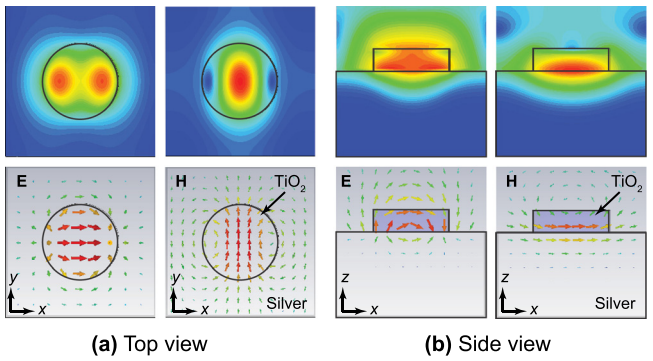

FIG. 3. Numerically resolved instantaneous field distribution with an x-polarized plane wave excitation. (a) Top view and (b) side view for the electric field **E** and magnetic field **H** distributions, represented as vectors and colormap.

perfect electric conductor, at optical frequencies the electric field can penetrate into the metal and couple with collective electron oscillations or surface plasmons, as observable from Fig. 3(b). This effect prevents a direct scaling behavior of the optical dielectric resonators by reducing the size of dielectric resonators.[7]

The far-field spectral and angular response of the metasurface can be analyzed by using grating and array theories. According to the diffraction theory,[16] the response of a single grating element (sub-array) is convolved with the grating arrangement in the near-field. This convolution in the near-field translates into the product of the two angular responses after Fourier transformation into the far-field.

Grating: In the realized metasurface, the periodicity Λ is defined by the sub-arrays arrangement, i.e., $\Lambda = 1.86$ μm for the considered 6-element sub-array. The pattern of this grating is calculated independently using the array factor as defined in antenna theory.[19] This results in a first order diffraction towards 19.9° at the wavelength of 633 nm, which corresponds to the designed deflection angle according to the reflectarray theory Eq. (1). The spectral far-field behavior of this grating is shown in Fig. 4(a), where the grating lobes or diffraction orders $m = -1$, 0, and $+1$ are clearly identified. The results are shown here for an arrangement of $N = 5$ periodic repetitions and the diffracted beam width will decrease with an increase in the aperture size, i.e., the number of sub-arrays. Side lobes characteristic of antenna arrays are clearly observed when using a plane wave excitation.

Far-field pattern of a single sub-array: In the simulation with the Lumerical FDTD Solutions software, one sub-array composed of the six resonators with periodic boundaries is excited with a wide band plane wave at normal incidence. The spectral scattering behavior of a single sub-array is shown in Fig. 4(b). Using the terminology of antenna technology, the represented pattern is the so-called "embedded patterns," i.e., it is retrieved for a single element (sub-array) embedded in an infinite periodic arrangement that is responsible for edge coupling. In other words, periodic boundaries are utilized to maintain the same coupling for the first and last resonators. The far-field pattern in Fig. 4(b) is the contribution of one such sub-array. The sub-array pattern shows a deflected beam pointing towards around 20° at the targeted wavelength, where the elements size are chosen according to

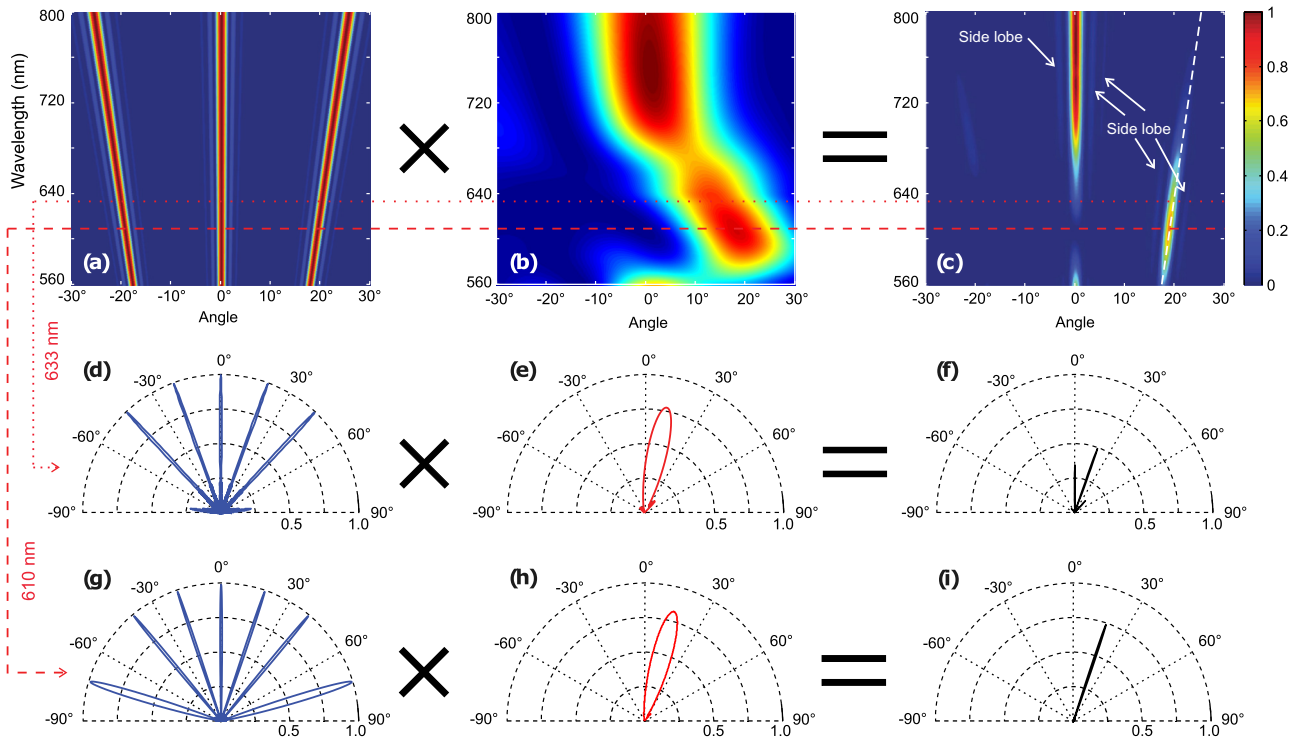

FIG. 4. Simulated reflected power of (a) the grating with $\Lambda = 1.86\ \mu$m, (b) a single 6-element dielectric resonator sub-array with a pitch of 310 nm, and (c) the multiplication of (a) and (b). (d)–(f) and (g)–(i) Corresponding angular patterns at 633 nm and 610 nm, respectively. The reflection is normalized to the maximum reflected power from the silver surface.

the curve of Fig. 1(a). At longer wavelengths, most of the elements will be far from resonance and in the flat part of the phase curve, and thus specular reflection will become dominant.

Far-field pattern of a finite repetition of sub-arrays: The multiplication of the scattering pattern of a single sub-array with the finite grating behavior results in the overall metasurface response shown in Fig. 4(c). This periodic arrangement can be interpreted, in principle, as a blazed diffraction grating.[16] The behavior of the metasurface is however different from a conventional grating, in the sense that the angular scattering response of the individual sub-arrays of *discrete* elements is superimposed to the grating response.

In the present case, as shown in Fig. 4(c), the best performance of the gradient metasurface occurs for maximum ratio of deflection to reflection. This is observed at the wavelength of 610 nm instead of the desired 633 nm. The corresponding angular patterns at 633 nm and 610 nm are shown in the second row of Figs. 4(d)–4(f) and third row of Figs. 4(g)–4(i), respectively. This discrepancy of a few percent can be attributed to coupling effects: The phase curve in Fig. 1(b) is obtained from infinite uniform arrays, whereas in the actual metasurface design, a difference in the diameter of adjacent dielectric resonators influences the inter-element coupling between dielectric resonators. This effect introduces, as a result, a slight phase offset for each dielectric resonator, compared to the phase obtained in an infinite uniform array. This phase offset causes the optimal operation to slightly deviate from the designed wavelength. In order to reduce the impact from the coupling effects, the metasurface is illuminated with TE polarized light, i.e., the **E** field is aligned along the x axis in Fig. 2(a). For a given dielectric resonator array, the coupling between resonators is significant in the **E** field direction.[25] However, since the diameter of resonators on the metasurface is uniform along the x axis, the coupling effect is similar to that in the uniform array, and hence, the local phase response and far-field performance are reasonably preserved. A slightly decreased performance is observed when the metasurface is illuminated with TM-polarized light. A final optimization of the local phase responses in the subarray design can increase the efficiency further by compensating coupling effects.

To validate the simulation results, the spectral behavior of the metasurface has been measured under white TE polarized light illumination, at the back focal plane of a

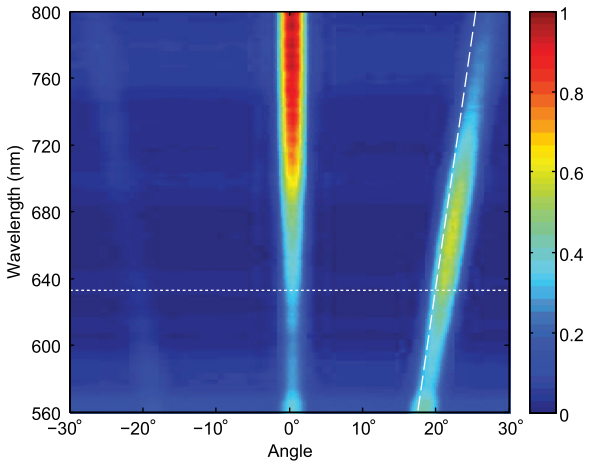

FIG. 5. Spectral measurement of the reflectance of the dielectric resonator metasurface. The white dotted and dashed lines indicate the wavelength of 633 nm and the calculated deflection angle θ using Eq. (1).

microscope setup.[20] In Fig. 5, the measured result has been calibrated with the reflection from a mirror to obtain the same incident power over all wavelengths. The white dashed line indicates the deflection angle θ calculated by using Eq. (1). The measured angle is slightly larger than predicted because the realized lattice of about 300 nm is slightly smaller than the desired lattice of 310 nm, as shown in Fig. 2(b). The beam width observed in the experiment is broader than that from the simulation. A plane wave illumination is employed in the simulation, while the metasurface is illuminated by a Gaussian beam in the experiment. This nonuniform illumination (which resembles a low-side lobe distribution in array theory) increases the beam width, while decreasing the side lobe level. The best performance of the metasurface moves to the wavelength of 650 nm due to the fabrication imperfection, i.e., a variation in the size and lattice constant of corresponding resonators in each sub-array. The reflectance pattern at wavelength of 633 nm shows that around 50% power has been deflected towards an angle of about 20°.

In conclusion, we have experimentally observed the spectral and angular responses of the gradient metasurface made of dielectric resonators with a linearly varying phase response. The diffraction theory and equivalently the array theory have been applied to analyze the observed response of this metasurface. The far-field response of the metasurface corresponds to the multiplication of the single subarray response with the grating response. The analysis and results offer generic understanding towards the behavior of periodic gradient metasurfaces.

C.F. acknowledges the ARC Future Fellowship funding scheme under FT100100585. M.K. acknowledges the support of the UKs Engineering and Physical Sciences Research Council (EPSRC), Cross-Disciplinary Interfaces Programme (C-DIP) Fellowship Fund, Grant EP/I017852/1. M.B. and S.S. acknowledge Australian Post-Doctoral Fellowships through ARC Discovery Projects DP1092717 and DP110100262, respectively.

[1]N. Yu and F. Capasso, "Flat optics with designer metasurfaces," Nat. Mater. **13**, 139–150 (2014).
[2]C. Pfeiffer and A. Grbic, "Millimeter-wave transmitarrays for wavefront and polarization control," IEEE Trans. Microwave Theory Tech. **61**, 4407–4417 (2013).
[3]D. Schurig, J. J. Mock, B. J. Justice, S. A. Cummer, J. B. Pendry, A. F. Starr, and D. R. Smith, "Metamaterial electromagnetic cloak at microwave frequencies," Science **314**, 977–980 (2006).
[4]C. Holloway, E. F. Kuester, J. Gordon, J. O'Hara, J. Booth, and D. Smith, "An overview of the theory and applications of metasurfaces: The two-dimensional equivalents of metamaterials," IEEE Antennas Propag. Mag. **54**, 10–35 (2012).
[5]A. V. Kildishev, A. Boltasseva, and V. M. Shalaev, "Planar photonics with metasurfaces," Science **339**, 1232009 (2013).
[6]J. Huang and J. Encinar, *Reflectarray Antennas* (Wiley-IEEE Press, 2007).
[7]L. Zou, W. Withayachumnankul, C. Shah, A. Mitchell, M. Klemm, M. Bhaskaran, S. Sriram, and C. Fumeaux, "Efficiency and scalability of dielectric resonator antennas at optical frequencies," IEEE Photonics J. **6**, 1–10 (2014).
[8]I. Staude, A. E. Miroshnichenko, M. Decker, N. T. Fofang, S. Liu, E. Gonzales, J. Dominguez, T. S. Luk, D. N. Neshev, I. Brener, and Y. Kivshar, "Tailoring directional scattering through magnetic and electric resonances in subwavelength silicon nanodisks," Nano Lett. **7**, 7824–7832 (2013).
[9]F. Bigourdan, F. Marquier, J.-P. Hugonin, and J.-J. Greffet, "Design of highly efficient metallo-dielectric patch antennas for single-photon emission," Opt. Express **22**, 2337–2347 (2014).
[10]L. Zou, W. Withayachumnankul, C. Shah, A. Mitchell, M. Bhaskaran, S. Sriram, and C. Fumeaux, "Dielectric resonator nanoantennas at visible frequencies," Opt. Express **21**, 1344–1352 (2013).
[11]D. S. Filonov, A. E. Krasnok, A. P. Slobozhanyuk, P. V. Kapitanova, E. A. Nenasheva, Y. S. Kivshar, and P. A. Belov, "Experimental verification of the concept of all-dielectric nanoantennas," Appl. Phys. Lett. **100**, 201113 (2012).
[12]J. van de Groep and A. Polman, "Designing dielectric resonators on substrates: Combining magnetic and electric resonances," Opt. Express **21**, 26285–26302 (2013).
[13]J. C. Ginn, I. Brener, D. W. Peters, J. R. Wendt, J. O. Stevens, P. F. Hines, L. I. Basilio, L. K. Warne, J. F. Ihlefeld, P. G. Clem, and M. B. Sinclair, "Realizing optical magnetism from dielectric metamaterials," Phys. Rev. Lett. **108**, 097402 (2012).
[14]Y. Yang, W. Wang, P. Moitra, I. I. Kravchenko, D. P. Briggs, and J. Valentine, "Dielectric meta-reflectarray for broadband linear polarization conversion and optical vortex generation," Nano Lett. **14**, 1394–1399 (2014).
[15]L. Zou, M. Cryan, and M. Klemm, "Phase change material based tunable reflectarray for free-space optical inter/intra chip interconnects," Opt. Express **22**, 24142–24148 (2014).
[16]S. Larouche and D. R. Smith, "Reconciliation of generalized refraction with diffraction theory," Opt. Lett. **37**, 2391–2393 (2012).
[17]T. Niu, W. Withayachumnankul, B. S.-Y. Ung, H. Menekse, M. Bhaskaran, S. Sriram, and C. Fumeaux, "Experimental demonstration of reflectarray antennas at terahertz frequencies," Opt. Express **21**, 2875–2889 (2013).
[18]K. M. Luk and K. W. Leung, *Dielectric Resonator Antennas* (Research Studies Press Ltd. England, 2003).
[19]C. Balanis, *Antenna Theory: Analysis and Design*, 3rd ed. (Wiley, 2005).
[20]M. López-García, J. F. Galisteo-López, A. Blanco, J. Sánchez-Marcos, C. López, and A. García-Martín, "Enhancement and directionality of spontaneous emission in hybrid self-assembled photonic-plasmonic crystals," Small **6**, 1757–1761 (2010).
[21]Q. Lai, G. Almpanis, C. Fumeaux, H. Benedickter, and R. Vahldieck, "Comparison of the radiation efficiency for the dielectric resonator antenna and the microstrip antenna at Ka band," IEEE Trans. Antennas Propag. **56**, 3589–3592 (2008).
[22]C. Pfeiffer, N. K. Emani, A. M. Shaltout, A. Boltasseva, V. M. Shalaev, and A. Grbic, "Efficient light bending with isotropic metamaterial Huygens surfaces," Nano Lett. **14**, 2491–2497 (2014).
[23]S. Sun, K.-Y. Yang, C.-M. Wang, T.-K. Juan, W. T. Chen, C. Y. Liao, Q. He, S. Xiao, W.-T. Kung, G.-Y. Guo, L. Zhou, and D. P. Tsai, "High-efficiency broadband anomalous reflection by gradient meta-surfaces," Nano Lett. **12**, 6223–6229 (2012).
[24]N. Yu, P. Genevet, M. A. Kats, F. Aieta, J.-P. Tetienne, F. Capasso, and Z. Gaburro, "Light propagation with phase discontinuities: Generalized laws of reflection and refraction," Science **334**, 333–337 (2011).
[25]C. Fumeaux, G. Almpanis, K. Sankaran, D. Baumann, and R. Vahldieck, "Finite-volume time-domain modeling of the mutual coupling between dielectric resonator antennas in array configurations," in *The Second European Conference on Antennas and Propagation* (2007), pp. 1–4.